

# LncRNA-miRNA-mRNA Network Analysis Reveals the Potential Biomarkers in Crohn's Disease Rats Treated with Herb-Partitioned Moxibustion

Xue-Jun Wang<sup>1,\*</sup>, Xiao-Ying Li<sup>1,\*</sup>, Xiao-Cong Guo<sup>1,\*</sup>, Li Liu<sup>1</sup>, You-You Jin<sup>1</sup>, Yun-Qiong Lu<sup>1</sup>, Yao-Jia-Ni Cao<sup>1</sup>, Jun-Yi Long<sup>1</sup>, Huan-Gan Wu<sup>2</sup>, Dan Zhang<sup>2</sup>, Guang Yang<sup>2</sup>, Jue Hong<sup>2</sup>, Yan-Ting Yang<sup>2</sup>, Xiao-Peng Ma<sup>1,2</sup>

<sup>1</sup>Yueyang Hospital of Integrated Traditional Chinese and Western Medicine, Shanghai University of Traditional Chinese Medicine, Shanghai, People's Republic of China; <sup>2</sup>Key Laboratory of Acupuncture-Moxibustion and Immunology, Shanghai Research Institute of Acupuncture and Meridian, Shanghai, People's Republic of China

\*These authors contributed equally to this work

Correspondence: Xiao-Peng Ma; Yan-Ting Yang, Key Laboratory of Acupuncture-Moxibustion and Immunology, Shanghai Research Institute of Acupuncture and Meridian, Shanghai, People's Republic of China, Email pengpengma@163.com; tcmyyt@126.com

**Background:** Long noncoding RNA (lncRNA) is receiving growing attention in Crohn's disease (CD). However, the mechanism by which herb-partitioned moxibustion (HPM) regulates the expression and functions of lncRNAs in CD rats is still unclear. The aim of our study is to identify lncRNA-miRNA-mRNA network potential biological functions in CD.

**Methods:** RNA sequencing and microRNA (miRNA) sequencing were carried out to analyze lncRNA, miRNA and mRNA expression profiles among the CD rats, normal control rats, and CD rats after HPM treatment and constructed the potential related lncRNA-miRNA-mRNA competing endogenous RNA (ceRNA) networks. Then, Gene Ontology (GO), Kyoto Encyclopedia of Genes and Genomes (KEGG) pathway enrichment analysis, protein-protein interaction (PPI) analysis and quantitative real-time polymerase chain reaction (qRT-PCR) were performed to explore potentially important genes in ceRNA networks.

**Results:** A total of 189 lncRNAs, 32 miRNAs and 463 mRNAs were determined as differentially expressed (DE) genes in CD rats compared to normal control rats, and 161 lncRNAs, 12 miRNAs and 130 mRNAs were identified as remarkably DE genes in CD rats after HPM treatment compared to CD rats. GO analysis indicated that the target genes were most enriched in cAMP and in KEGG pathway analysis the main pathways included adipocytokine, PPAR, AMPK, FoxO and PI3K-Akt signaling pathway. Finally, qRT-PCR results confirmed that lncRNA LOC102550026 sponged miRNA-34c-5p to regulate the intestinal immune inflammatory response by targeting Pck1.

**Conclusion:** By constructing a ceRNA network with lncRNA-miRNA-mRNA, PCR verification, and KEGG analysis, we revealed that LOC102550026/miRNA-34c-5p/Pck1 axis and adipocytokine, PPAR, AMPK, FoxO, and PI3K-Akt signaling pathways might regulate the intestinal immune-inflammatory response, and HPM may regulate the lncRNA LOC102550026/miR-34c-5p/Pck1 axis and adipocytokine, PPAR, AMPK, FoxO, and PI3K-Akt signaling pathways, thus improving intestinal inflammation in CD. These findings may be novel potential targets in CD.

**Keywords:** herb-partitioned moxibustion, Crohn's disease, lncRNA, ceRNA, lncRNA LOC102550026/miR-34c-5p/Pck1 axis

## Background

Crohn's disease (CD) is an inflammatory bowel disease that is characterized by chronic inflammatory disorder of the digestive tract, with a progressive and destructive course with accelerating incidence worldwide. CD lesions are often segmentally distributed, possibly affecting any part of the gastrointestinal tract.<sup>1,2</sup> Although the exact pathogenesis of CD

remains unknown, it contains a complex interplay between genetic susceptibility, environmental factors, and immune responses, in which the most rapid progress happens in genetics studies.<sup>3-5</sup>

Long non-coding RNA (lncRNA) is a class of transcripts that contain more than 200 nucleotides with low protein encoding potential.<sup>6,7</sup> Accumulating studies reported that the lncRNAs are considered as critical gene regulators in various biological processes, including cell proliferation and differentiation, development and inflammation.<sup>8-10</sup> lncRNAs contain microRNA (miRNA)-response elements, which function as a competitive endogenous RNA (ceRNA), interacting with miRNAs to indirectly regulate mRNAs.<sup>11,12</sup> Specifically, lncRNAs are found to be significantly involved in inflammatory diseases, such as rheumatoid arthritis, ankylosing spondylitis and osteoarthritis.<sup>13-15</sup> As for CD, increasing studies suggest that lncRNA plays a crucial role in the pathogenesis.<sup>16</sup> For example, lncRNA DQ786243 can be connected with the severity of CD, and it affects the expression of CREB and Foxp3 via regulating the function of Treg.<sup>17</sup> Yael showed that lncRNA LINC01272 is related to a myeloid pro-inflammatory signature, whereas lncRNA HNF4A-AS1 is associated with an epithelial metabolic signature.<sup>18</sup> Another study reported that lncRNA MALAT1 as a ceRNA maintains the intestinal mucosal homeostasis via the miR-146b-5p-CLDN11/NUMB pathway in CD.<sup>19</sup>

Herb-partitioned moxibustion (HPM) has been reported to treat CD as an effective alternative therapy and verified to achieve positive therapeutic effects.<sup>20</sup> HPM can regulate A20 expression to protect the intestinal epithelial tight junctions and repair the damage of intestinal epithelial barrier in CD mice.<sup>21,22</sup> Another study illustrated that HPM inhibited colonic epithelial cell apoptosis by regulating the TNF-alpha and TNFR1 expressions in CD model rats.<sup>23</sup> Furthermore, autophagy and immune-associated gene expressions in colon tissues of CD rats are influenced by HPM to decrease intestinal inflammation and promote the repair of colonic mucosa.<sup>24</sup> However, whether HPM can regulate lncRNAs in CD development and progression is still vastly unknown, and the role of HPM in regulating ceRNA in the development of CD has not been comprehensively explored. Therefore, it is important to explore whether HPM can regulate ceRNA in the development of CD.

In this study, we detected the colonic mucosal lncRNA, miRNA and mRNA expression profiles by RNA sequencing in CD rats, normal control rats, and CD rats after HPM treatment and constructed the potentially related lncRNA-miRNA-mRNA networks. A series of analyses were used to explore potentially important genes involved in CD. Furthermore, qRT-PCR was performed to validate the expression of the lncRNAs/miRNAs/mRNAs. Our study aims to provide beneficial information about understanding the development of CD and the mechanism of HPM treatment from lncRNA-miRNA-mRNA network analysis.

## Materials and Methods

### Animals and Experimental Grouping

A total of 27 Sprague-Dawley rats (150±20 g) were obtained from Shanghai SLAC Laboratory Animal Co., Ltd. (Shanghai, China; License no: SCXK (Shanghai) 2017-0005). The rats were raised at Yueyang Clinical Medicine School, Shanghai University of Traditional Chinese Medicine, and randomly divided into three groups, with 9 rats in each group: the normal control group (NG), model group (MG), herb-partitioned moxibustion group (HPMG). All protocols for animal experiments were performed in strict accordance with the International Guiding Principles for Biomedical Research Involving Animals recommended by the World Health Organization and were approved by the Animal Care and Use Committee of Shanghai University of Traditional Chinese Medicine.

### Animal Model

Rat model of TNBS-induced CD was established according to the previous study.<sup>25</sup> The NG was fed routine chow, and the CD model was induced from MG and HPMG by administration of an enema containing a mixture of TNBS and ethanol.<sup>25</sup> Briefly, before model establishment, all rats were fasted and given only water for 24 h, weighed and anaesthetized using an intraperitoneal injection of 1% pentobarbital sodium (45 mg/kg). The TNBS mixture was slowly instilled into the intestinal cavity with a rubber cannula (3 mL/kg), and TNBS was administered. The rats were inverted for 1 min. The procedure was repeated every 7 days for 4 weeks. After the modeling process was completed, one animal from each group was randomly

selected for H&E staining of colon tissue to determine whether the CD model was successfully established. Only after the successful establishment of the model, follow-up interventions were carried out. The animal protocols were approved by the Ethics Committee of Yueyang Clinical Medicine School, Shanghai University of Traditional Chinese Medicine (No. YYLAC-2020-085).

## Treatment

In the HPMG, treatment was administered by placing a moxa cone on the top of an herbal cake at the Tianshu (ST25, bilateral) and Qihai (CV6) points and igniting it (Figure 1). The treatment lasted for 10 min once daily for 7 days. The herbal cake was a thick paste made of Chinese medicine powder (aconite). The moxa cone was made by placing approximately 90 mg moxa wool in a mold (0.6 cm in diameter and 0.6 cm high). The rats in the NG and MG did not receive any treatment.

## Sample Collection and Processing

After the intervention, all rats were anesthetized by intraperitoneal injection of 2% pentobarbital sodium (45 mg/kg). All rats were immediately euthanized by abdominal aorta exsanguination just after loss of consciousness. Then, the abdominal cavity was opened and the length of the colon was recorded.<sup>26</sup> The colon was then opened longitudinally and weighed. Afterwards, the colon tissues were washed in PBS to clear fecal residues. Colon macroscopic damage indexes (CMDIs) were determined.<sup>27</sup> The scores are shown in [Supplementary Table 1](#). Afterwards, 6–8 cm of the distal colon was collected 2 cm from the anus. Each colon was divided into three parts: one part was fixed in 4% paraformaldehyde, and the other two parts were stored in a  $-80^{\circ}\text{C}$  freezer.

## Hematoxylin and Eosin (H&E) Staining

H&E was performed to assess colon injury and inflammation. The colon tissues were paraffin embedded and stained with H&E. Briefly, the slides were incubated with hematoxylin solution, eosin solution, 70% ethanol, 90% ethanol, 100% ethanol, and xylene. Finally, the sections were sealed and observed with a light microscope.

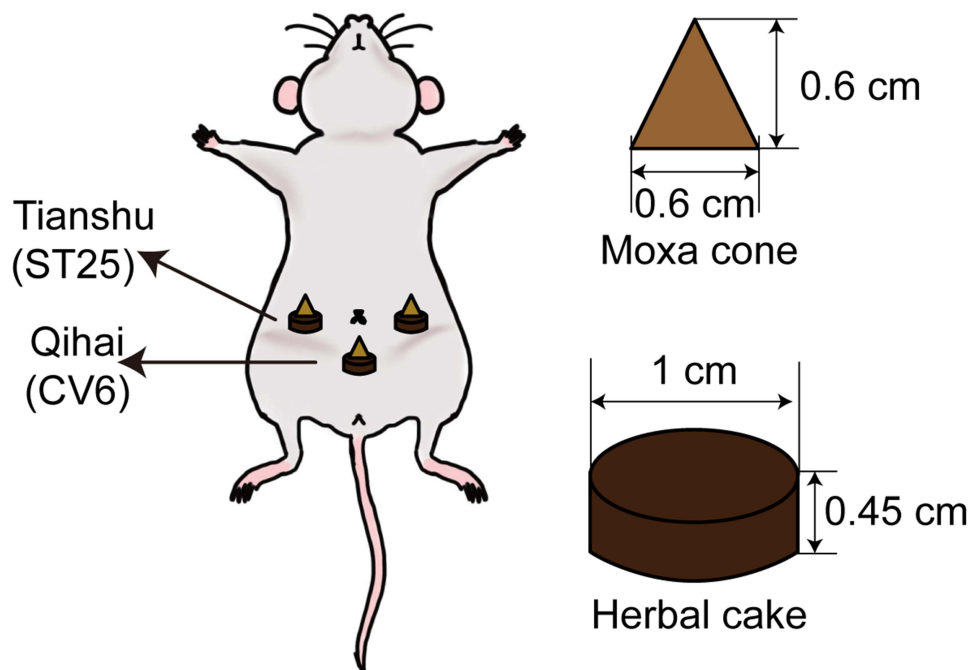


**Figure 1** Illustration of herb-partitioned moxibustion. HPM treatment was administered by placing a moxa cone on the top of an herbal cake at the Tianshu (ST25, bilateral) and Qihai (CV6) points and igniting it.

## RNA Isolation and Construction of RNA Library

Colon samples from all the three groups, normal control group, model group and herb-partitioned moxibustion group, were analyzed by high-throughput sequencing by Oebiotech Company (Shanghai, China) to detect lncRNA, mRNA and miRNA expression profiles. In brief, total RNA was isolated using mirVana™ miRNA Isolation Kit (Thermo). Afterward, the RNA integrity and concentration were determined by the Gel imaging system (Tanon 2500, Biotanon Co., Ltd) and the NanoDrop 2000 (Thermo). According to the protocol, the TruSeq Stranded Total RNA with Ribo-Zero Gold Prep Kit (Illumina) was used to construct lncRNA and mRNA libraries, and the TruSeq Small RNA Sample Prep Kits (Illumina) was used to construct small RNA libraries. For mRNA and lncRNA, RNA was purified by magnetic beads after removal of rRNA. Subsequently, the first-strand cDNA and second-strand cDNA were synthesized and library fragments were purified using AMPure XP beads to select cDNA fragments.

For miRNA, the 3' end of the miRNA was specifically ligated with 3' Adaptor, and the Super Script II Reverse Transcriptase was used to synthesize the first strand cDNA. It was used for PCR amplification with ultrapure water, PCR mix and RNA PCR primer. The DNA fragments within 147–157 bp of these amplification products were recovered by RNA gel electrophoresis, and the pieces were purified to establish a small RNA library by the Agilent Technologies 2100 Bioanalyzer. The sequencing data were deposited in a public repository (Sequence Read Archive, <https://www.ncbi.nlm.nih.gov/sra/PRJNA803616>).

## Bioinformatic Analysis of mRNA and lncRNA

StringTie software was used to count the fragment within each gene.<sup>28</sup> Then, transcripts with coding potential were screened out by Pfam, PLEK, CPC and CNCI to obtain lncRNA predicted sequences.<sup>29–31</sup> Aligning the sequencing reads of each sample with the sequence of mRNA transcript sequences, known lncRNA sequences and lncRNA prediction sequences were detected using Bowtie2. Gene quantitative analysis was conducted by eXpress, the fragments per kilobase of exon model per million reads mapped (FPKM) value and counts (the number of reads for each gene in each sample) were obtained. Estimate Size Factors function of the DESeq (2012) R package was used to normalize the counts, and nbinom Test function was performed to determine *p* value and fold change values for the difference comparison. The statistical significance was defined as *p*-values  $\leq 0.05$  and fold change  $\geq 2$ , and the Gene Ontology (GO) and Kyoto Encyclopedia of Genes and Genomes (KEGG) enrichment analysis were performed using Hypergeometric Distribution Test.

## Bioinformatic Analysis of miRNAs

Non-coding RNAs were marked as rRNAs, tRNAs, small nuclear RNAs (snRNAs), and small nucleolar RNAs (snoRNAs). These RNAs were aligned and then subjected to the BLAST<sup>32</sup> search against Rfam v.10.1 (<http://www.sanger.ac.uk/software/Rfam>)<sup>33</sup> and GenBank databases (<http://www.ncbi.nlm.nih.gov/genbank/>). Aligning against miRBase v.21 database (<http://www.mirbase.org/>) was compared to identify the known miRNAs,<sup>34</sup> and the known miRNA expression patterns in different samples were analyzed. Novel miRNA prediction was performed using mirdeep2 software.<sup>35</sup> The miRNAs expression was calculated using the transcripts per million (TPM) method.  $TPM = \frac{\text{number of reads compared to each miRNA}}{\text{the total number of sample comparison reads}} \times 10^6$ .<sup>36</sup> Afterwards, the corresponding miRNA star sequences were identified using the hairpin structure of a pre-miRNA and the miRBase database. Differentially expressed genes (DEGs) were identified when the threshold of *p* value  $< 0.05$ . While DEG algorithm in the R package was used to calculate the *p* value for experiment with biological replicates, and Audic Claverie statistic was used to calculate the *p* value for experiment without biological replicates.<sup>37</sup> Miranda software was used to predict the targets of differentially expressed (DE) miRNAs at the parameter as follows:  $S \geq 150$   $\Delta G \leq -30$  kcal/mol and demand strict 5' seed pairing. GO enrichment and KEGG pathway enrichment analysis of DE miRNA-target-gene were respectively performed using R based on the hypergeometric distribution.

## LncRNA-miRNA-mRNA Network Construction

Using Miranda v3.3a, regulatory relationships between lncRNAs and miRNAs and between miRNAs and mRNAs were predicted. Based on the lncRNAs and miRNAs interaction analysis and the miRNAs and mRNAs interaction analysis, the ceRNA networks were constructed and visualized using Cytoscape (version 3.6.1; <http://cytoscape.org/>).

## Protein-Protein Interaction (PPI) Analysis

We constructed a PPI network by an online search tool to detect the interacting genes/proteins (STRING) (<https://www.string-db.org/>).<sup>38</sup> According to PPI network, interactions between proteins translated were identified from mRNAs in the ceRNA network.

## Quantitative Real-Time Polymerase Chain Reaction (qRT-PCR)

The total RNA from the colon was isolated using EZ-press RNA Purification Kit (EZBioscience, USA). To measure the lncRNA and mRNA expression level, total RNA was used for cDNA synthesis using a PrimeScript™ RT Master Mix kit Perfect Real Time (Takara, Japan). The resultant cDNA was amplified at Roche Light Cycler 480 using SYBR® Premix Ex Taq™ II Tli RNaseH Plus (Takara, Japan). To measure the miRNA expression level, total RNA was converted into cDNA using EZ-press microRNA Reverse Transcription Kit (EZBioscience, USA), and the reactions were performed at Roche Light Cycler 480 using EZ-press microRNA qPCR Kit (EZBioscience, USA). The relative gene expression was analyzed using the  $2^{-\Delta\Delta C_t}$  method. To normalize the data, internal reference was used with U6 for miRNA, ACTIN for lncRNA and mRNA. The primer sequences are listed in [Supplementary Table 2](#).

## Western Blotting (WB)

Total protein was extracted from colon tissues. Protein samples were subjected to SDS PAGE gel and then transferred to PVDF membranes. Subsequently, Primary antibodies of Pck1 (Cell Signaling Technology, MA, USA) and  $\beta$ -actin (Beyotime, Shanghai, China) are used to incubate with PVDF membranes overnight at 4 °C. The next day, the membrane were incubated with HRP-conjugated secondary antibody (1:1000). The proteins were detected via the enhanced chemiluminescence kit (Beyotime, Shanghai, China). ImageJ software was used to analyze the gray values of the proteins.

## Statistical Analysis

All the data (except for the CMDIs score) were presented as mean  $\pm$  standard deviation (SD) and were analyzed by one-way ANOVA with Bonferroni's multiple comparison test. qRT-PCR (lncRNA LOC102557338, miR-34a-5p, miR-34c-5p, Pck1 and pdzklip1 mRNA) results were analyzed by the least significant difference (LSD) test. qRT-PCR (lncRNA LOC102550026) results were analyzed by the Games-Howell test. CMDI data were expressed as median ( $P_{25}$ ,  $P_{75}$ ) and analyzed by the nonparametric Kruskal-Wallis  $H$ -test.  $P_{adj} < 0.05$  was considered statistically significant. SPSS 25.0 (IBM, Armonk, NY, United States) and GraphPad Prism 8.0 software were used.

## Results

### General Condition and Histological Analysis

The CMDIs varied significantly among different groups. The CMDIs in the MG were distinctly increased compared with those in the NG (Figure 2A;  $P < 0.001$ ). After treatment, the scores were reduced in the HPMG (Figure 2A) ( $P < 0.05$  vs the MG). Compared with the NG, the colons of rats in the MG were significantly shorter (Figure 2B and C) ( $P < 0.001$ ). In contrast, the colons of rats in the HPMG were considerably longer (Figure 2B and C) ( $P < 0.01$  vs the MG).

The rat colon showed no specific histological damage in the NG (Figure 2D). But in the MG (Figure 2E), colon injury was severe: mucosal glands destruction, a large number of inflammatory cells infiltrating into the mucosa and submucosa, vasodilation and hyperemia, fissure-like ulcer formation, and severe abnormal morphological changes were observed. In the HPMG (Figure 2F), epithelial tissue was repaired, with slight edema and inflammatory cells infiltrated into the

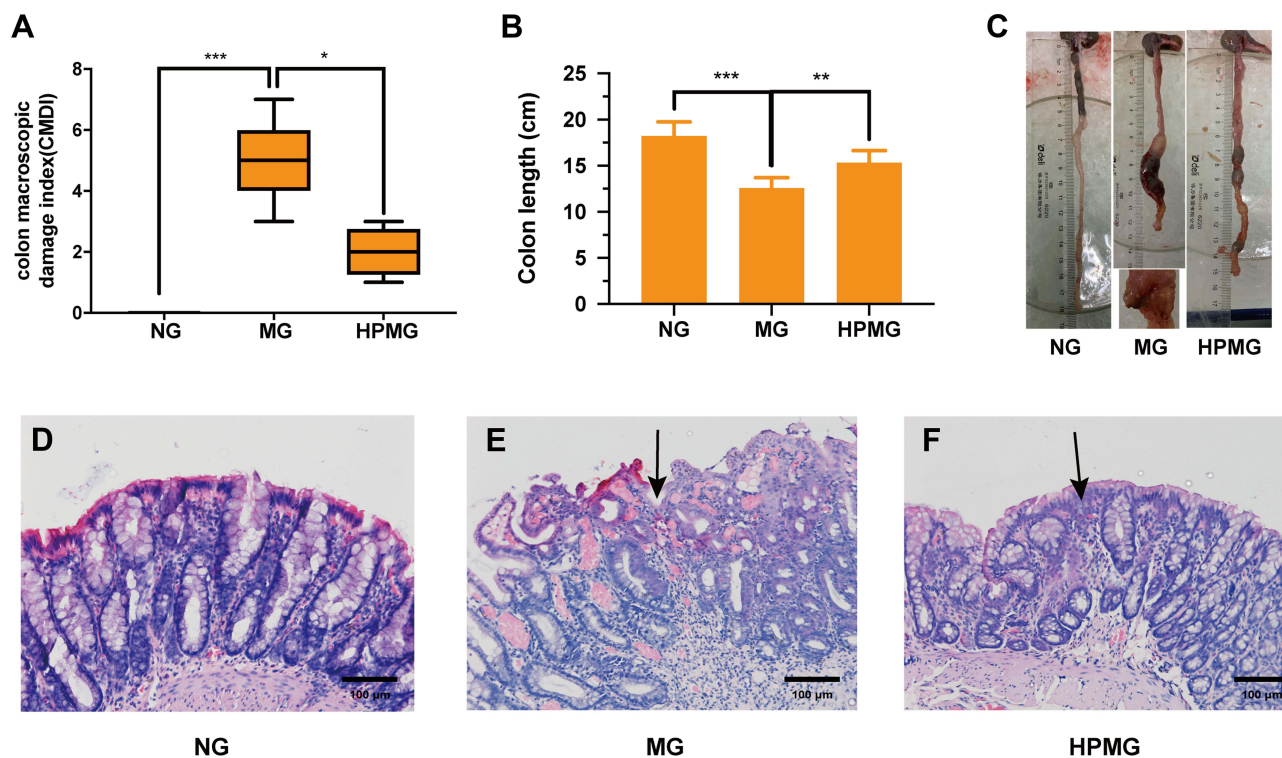


**Figure 2** CMDIs, colon length and morphological observation. **(A)** CMDIs. **(B)** Colon length. **(C)** Colon images. **(D–F)** Morphological observation with hematoxylin and eosin (H&E) staining. Data are presented as the median ( $P_{25}$ ,  $P_{75}$ ) in **(A)** and mean  $\pm$  SD in **(B)**. \* $P < 0.05$ , \*\* $P < 0.01$ , \*\*\* $P < 0.001$ . The black arrow indicates the location of the ulcer. Scale bar: 100  $\mu$ m,  $n = 8$ .

**Abbreviations:** NG, normal control group; MG, model group; HPMG, herb-partitioned moxibustion group.

mucosa and submucosa, small ulcers were healed, and mild abnormal morphological changes were observed. These results indicated that HPM treatment can relieve colon injury and help with colon shortening in CD rats.

### Analysis of lncRNA Expression Profiles Between CD and Normal Control Rats

Differentially expressed lncRNAs in colon tissues from three NG and three MG rats were screened by RNA sequencing. As shown in [Figure 3A](#) and [B](#), the R package identified 189 DE lncRNAs ( $\log_2FC > 1$ ,  $P < 0.05$ ), including 89 upregulated and 100 downregulated lncRNAs in the MG compared to the NG. [Supplementary Table 3](#) presents the top 10 most significantly upregulated and downregulated lncRNAs differentially expressed in the MG, respectively.

To further investigate the relationship between lncRNAs and gene transcription regulation, we analyzed the GO clustering and KEGG pathway enrichment of DE lncRNAs. GO enrichment analysis disclosed that DE lncRNAs in the MG were enriched in the biological process (such as lung ciliated cell differentiation, negative regulation of mesenchymal cell proliferation involved in lung development and negative regulation of epithelial cell proliferation involved in lung morphogenesis), the cellular components (such as the cerebellar mossy fiber, polysomal ribosome and mitochondrial matrix), and the molecular function (such as RNA polymerase II transcription corepressor activity, protein tyrosine phosphatase activity and double-stranded DNA binding) ([Figure 3C](#)). The KEGG pathways were mainly related to hepatocellular carcinoma, PI3K–Akt signaling pathway, mTOR signaling pathway, NF–kappa B signaling pathway, Ras signaling pathway, and purine metabolism ([Figure 3D](#)). Together, these data indicated that the lncRNAs play a critical role in CD pathogenesis.

### Analysis of lncRNA Expression Profiles Between HPM and CD Rats

After HPM treatment, the DE lncRNAs in colon tissues from three MG and three HPMG rats were screened by RNA sequencing. A total of 161 DE lncRNAs were defined from the HPMG compared to the MG ( $\log_2FC > 1$ ,  $P < 0.05$ ), including 88 upregulated lncRNAs and 73 downregulated lncRNAs ([Figure 4A](#) and [B](#)). Top 10 upregulated and downregulated lncRNAs in the HPMG compared with the MG are listed in [Supplementary Table 4](#).

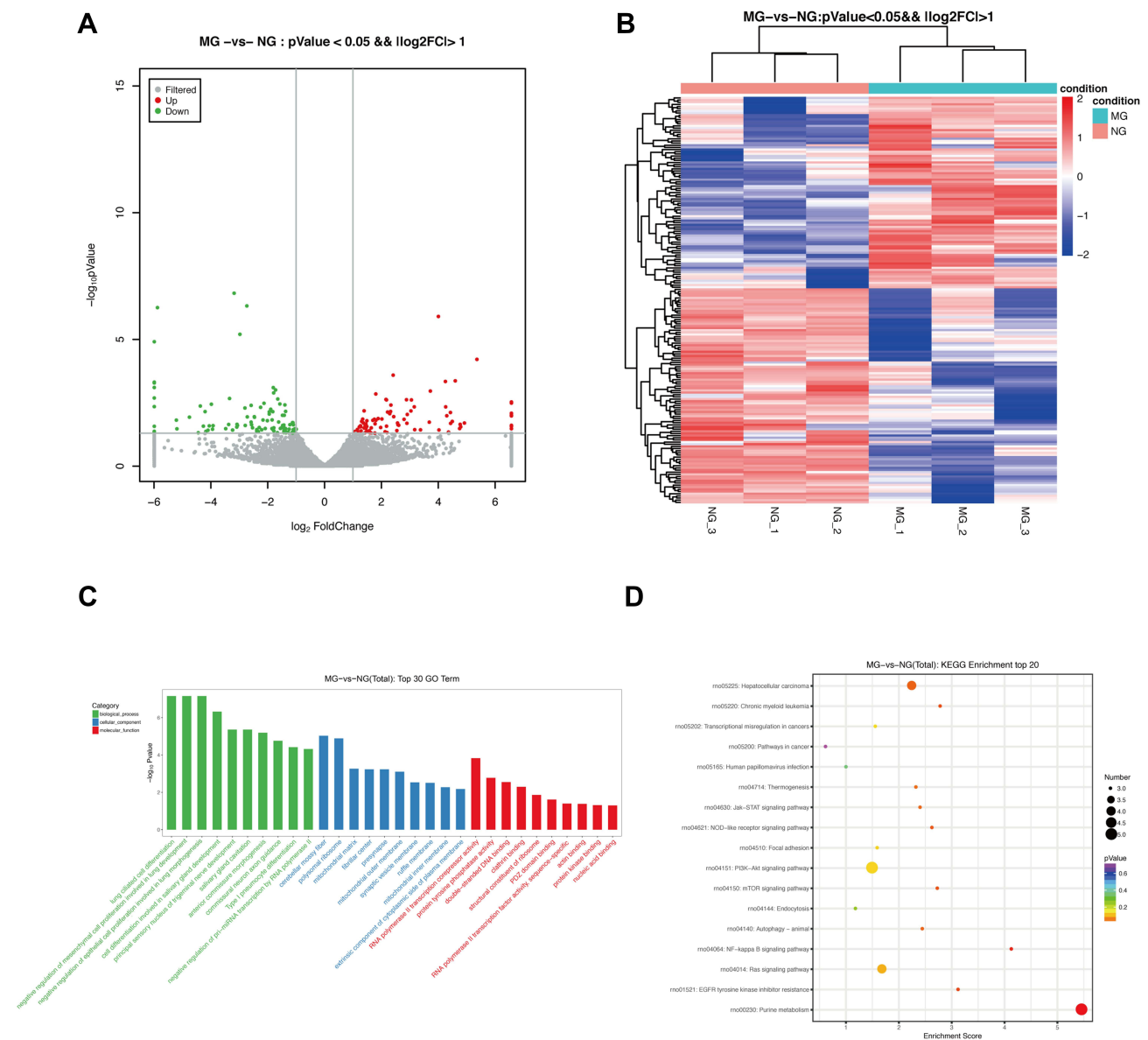


**Figure 3** The DE lncRNAs were analyzed based on the RNA sequencing data in MG and NG. **(A)** Volcano plot and **(B)** heatmap of DE lncRNAs between MG and NG ( $\log_2FC > 1$  and  $P < 0.05$ ). **(C)** Top 30 GO terms from the genes enrichment analysis and **(D)** top 20 significant KEGG pathways between MG and NG. **Abbreviations:** DE, differentially expressed; NG, normal control group; MG, model group; HPMG, herb-partitioned moxibustion group.

GO enrichment analysis disclosed that DE lncRNAs in the HPMG were enriched in the biological process (such as positive regulation of TOR signaling, lamellipodium assembly and receptor-mediated endocytosis), the cellular components (such as lamellipodium, growth cone, extracellular matrix and lysosome) and the molecular function (such as polysaccharide binding, scavenger receptor activity, G-protein coupled receptor activity, ATPase binding and transmembrane signaling receptor activity) (Figure 4C). The KEGG pathways were mainly related to Fc gamma R-mediated phagocytosis, cell adhesion molecules (CAMs), PI3K-Akt signaling pathway, phagosome and endocytosis (Figure 4D). Therefore, these results reflect the potential mechanism of HPM treatment in CD rats by regulating lncRNAs.

### Analysis of miRNA and mRNA Expression Profiles

Differentially expressed miRNAs in colon tissues from three NG, three MG and three HPMG rats were screened by small RNA sequencing. With a  $\log_2$  fold change, 32 miRNAs in the MG were shown to be differentially expressed in colon tissues relative to the NG. Among them, 25 and 7 were up- and down-regulated, respectively (Figure 5A and B).

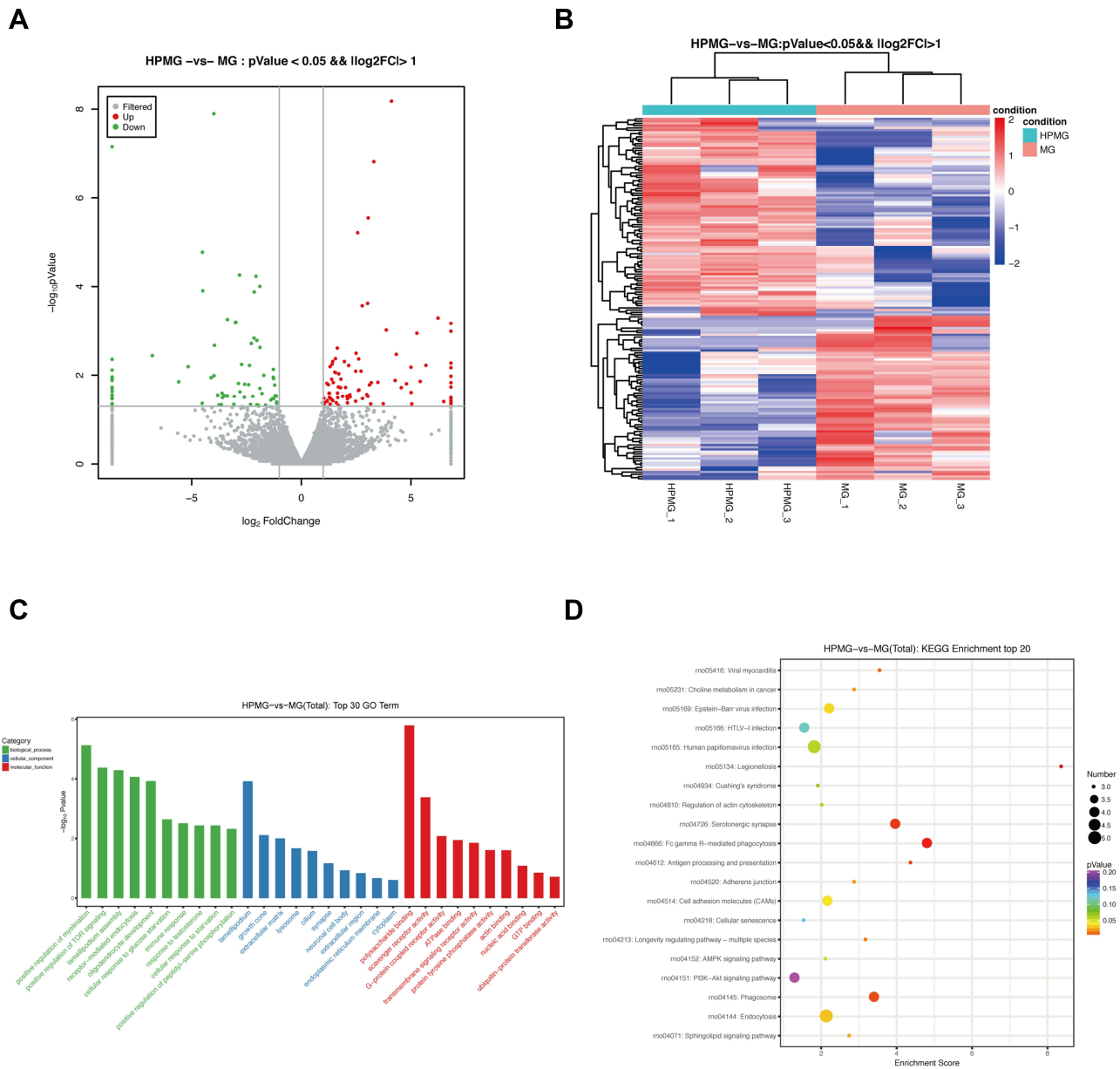


**Figure 4** The DE lncRNAs were analyzed based on the RNA sequencing data in HPMG and MG. **(A)** Volcano plot and **(B)** heatmap of DE lncRNAs between HPMG and MG ( $\log_2FC > 1$  and  $P < 0.05$ ). **(C)** Top 30 GO terms from the genes enrichment analysis and **(D)** top 20 significant KEGG pathways between HPMG and MG. **Abbreviations:** DE, differentially expressed; NG, normal control group; MG, model group; HPMG, herb-partitioned moxibustion group.

[Supplementary Table 5](#) presents the top 10 most significantly upregulated and 5 downregulated DE miRNAs in the MG, respectively. The potential functions of miRNA-related miRNAs in the MG by GO analysis and KEGG pathway analysis are listed in [Supplementary Figure 1](#).

With a  $\log_2$  fold change, the R package identified 12 DE miRNAs including 7 upregulated and 5 downregulated miRNAs in the HPMG compared to the MG ([Figure 5C](#) and [D](#)). [Supplementary Table 6](#) presents the 6 most significantly upregulated and 3 downregulated miRNAs differentially expressed in the HPMG, respectively. The potential functions of mRNA-related miRNAs in the HPMG by GO analysis and KEGG pathway analysis are listed in [Supplementary Figure 2](#).

We further explored differentially expressed mRNAs in colon tissues from three NG and three MG rats screened by RNA sequencing. As shown in [Figure 5E](#) and [F](#), the R package identified 463 DE mRNAs ( $\log_2FC > 1$ ,  $P < 0.05$ ), including 332 upregulated and 131 downregulated mRNAs in the MG compared to the NG. [Supplementary Table 7](#) presents the top 10 most significantly upregulated and downregulated mRNAs differentially expressed in the MG,



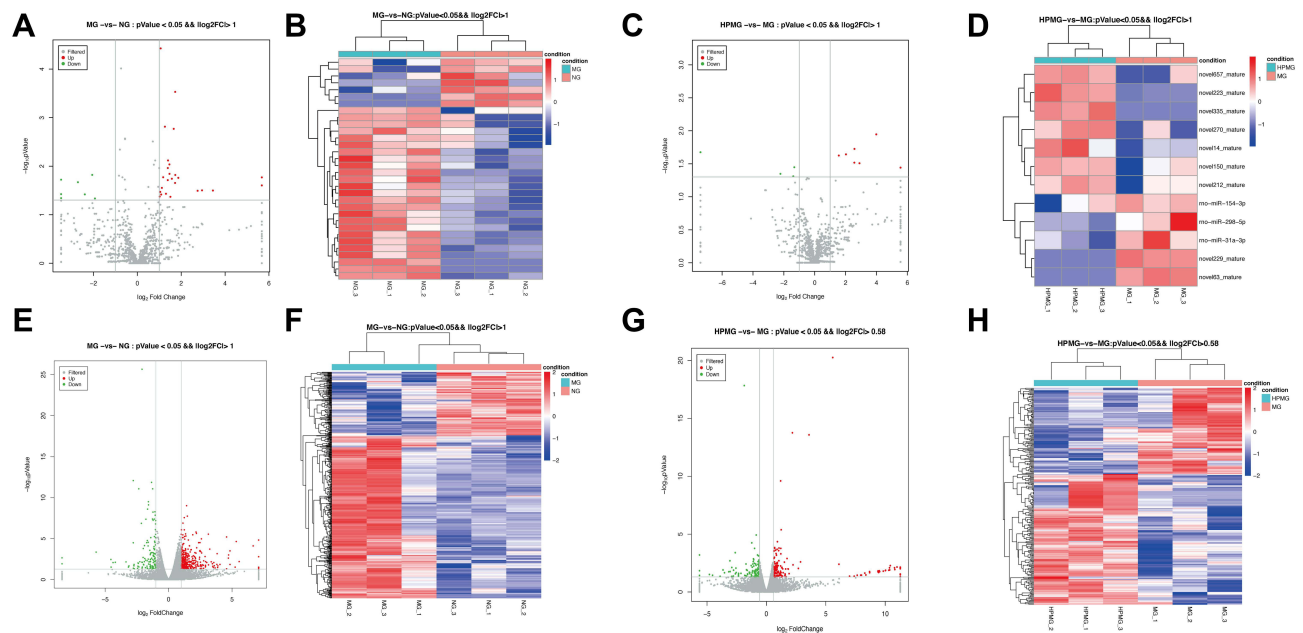


**Figure 5** The DE miRNAs and mRNAs were analyzed based on the small RNA and RNA sequencing data. (A) Volcano plot and (B) heatmap of DE miRNAs between MG and NG ( $\log_2FC > 1$  and  $P < 0.05$ ). (C) Volcano plot and (D) heatmap of DE miRNAs between HPMG and MG ( $\log_2FC > 1$  and  $P < 0.05$ ). (E) Volcano plot and (F) heatmap of DE mRNAs between MG and NG ( $\log_2FC > 0.58$  and  $P < 0.05$ ). (G) Volcano plot and (H) heatmap of DE mRNAs between HPMG and MG ( $\log_2FC > 0.58$  and  $P < 0.05$ ). **Abbreviations:** DE, differentially expressed; NG, control group; MG, model group; HPMG, herb-partitioned moxibustion group.

respectively. GO enrichment analysis and KEGG pathway analysis were performed to identify potential pathways or biological processes related to CD ([Supplementary Figure 3](#)).

After HPM treatment, DE mRNAs in colon tissues from three MG and three HPMG rats were screened by RNA sequencing. A total of 259 DE mRNAs were defined from the HPMG compared to MG ( $\log_2FC > 0.58$ ,  $P < 0.05$ ), including 156 upregulated mRNAs and 103 downregulated mRNAs ([Figure 5G](#) and [H](#)). Top 10 upregulated and downregulated mRNAs in the HPMG compared with MG are listed in [Supplementary Table 8](#). GO and KEGG analysis was completed to identify potential pathways or biological processes in the HPMG compared to the MG ([Supplementary Figure 4](#)).

## Establishment of lncRNA-miRNA-mRNA Network

To further illuminate the potential interactions of DE lncRNAs, miRNAs and mRNAs, we screened the co-expressed genes in the NG, MG, and HPMG rats, and performed ceRNA analysis to construct the lncRNA-miRNA-mRNA network. A total of 106 co-expressed lncRNAs, 29 co-expressed miRNAs and 382 co-expressed mRNAs were selected to perform ceRNA analysis. The miRNA-lncRNA and miRNA-mRNA regulatory pairs were analyzed using the Miranda v3.3a. In total, 33 miRNA-lncRNA regulatory pairs and 284 miRNA-mRNA regulatory pairs were identified. Based on the 200 mRNA-miRNA-lncRNA regulatory pairs among the top 100 mRNA-lncRNA pairs in the sorting results of the ceRNA analysis results, a ceRNA network was constructed ([Figure 6](#)).

To predict the roles of lncRNAs in lncRNA-associated ceRNA networks, GO and KEGG enrichment analyses were performed for coding genes directly interacting with lncRNAs. GO terms were enriched in the molecular function (such as transcription factor activity, transcription factor binding, cytoskeletal protein binding, FAT2 binding and cysteinyl leukotriene receptor activity), the cellular components (such as membrane-bounded organelle and cell body fiber), and the biological process (such as adenylate cyclase-modulating G-protein coupled receptor signaling pathway, cellular response to cAMP, cellular response to potassium ion starvation and N-acylethanolamine metabolic process) ([Figure 7A](#)). Whereas, in KEGG pathway analysis the main pathways included pyruvate metabolism, glutathione metabolism, glycolysis/gluconeogenesis, adipocytokine signaling pathway, PPAR signaling pathway, AMPK signaling pathway, FoxO signaling pathway and PI3K-Akt signaling pathway ([Figure 7B](#)).

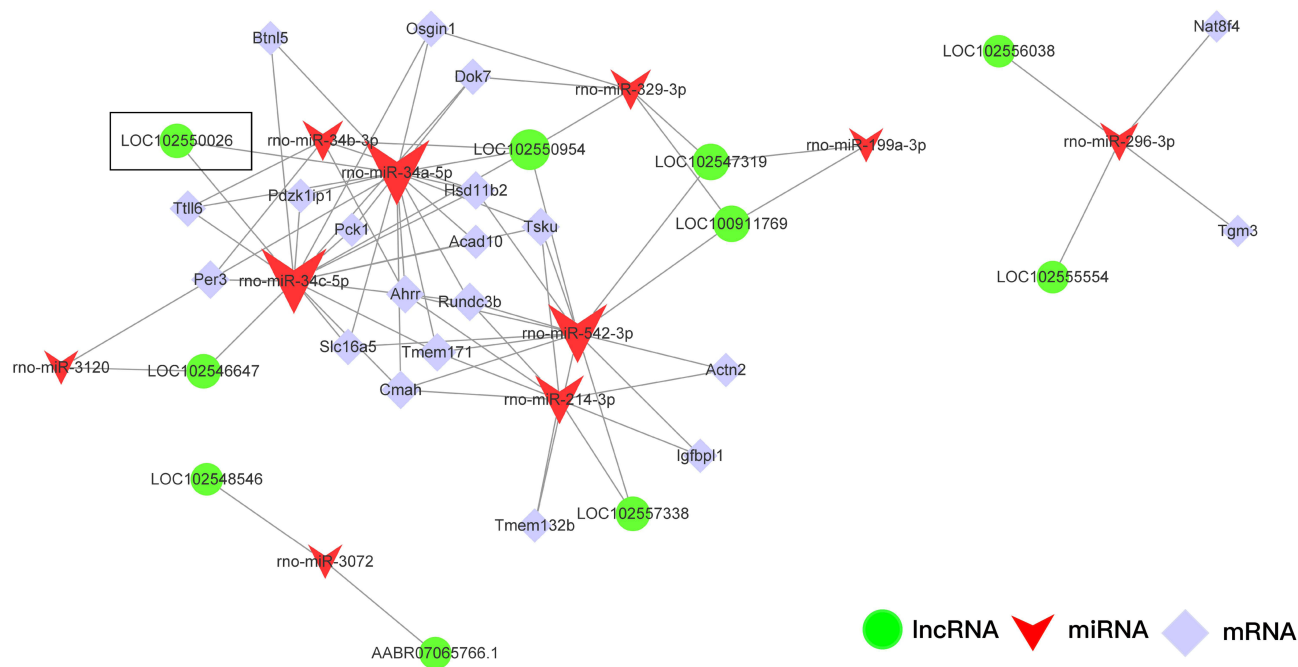


**Figure 6** LncRNA-miRNA-mRNA network analysis. Green, red and purple represent LncRNAs, miRNAs and mRNAs, respectively.

The interaction relationship between proteins was analyzed based on string database, and the network was constructed (Figure 7C). The centrality degree of each node was evaluated by the CentiScape plugin. 10 genes were defined as hub genes with the criterion, including Heyl, Per3, Hsd11b2, Pck1, Cmah, Prrx1, Osgin1, Acad10, Actn2 and Dok7 (Supplementary Table 9). Among them, Pck1 was the top one node centralized in net with the largest size (Figure 7C).

Together, these data indicated that the phosphoenolpyruvate carboxykinase 1 (Pck1)-mediated pyruvate metabolism, glycolysis/gluconeogenesis, and FoxO signaling pathways may be related to the pathogenesis of CD, and HPM may be able to exert anti-inflammatory effects by regulating Pck1 expression.

## Validation of RNA-Seq Results

The ceRNA network and functional analyses mentioned above, which were predicted to play important roles in NG, MG and HPMG, were validated by qRT-PCR. We selected the 2 lncRNAs with the highest ceRNA scores for validation. Compared with that in the NG, the lncRNA expression of LOC102550026 was significantly decreased in the MG ( $p < 0.05$ ), while the LOC102550026 expression level was markedly increased in the HPMG than in the MG ( $p < 0.05$ ) (Figure 8A). Compared with that in the NG, the lncRNA expression of LOC102557338 was significantly decreased in the MG ( $p < 0.05$ ), but the LOC102557338 expression level showed no significant difference in the HPMG than in the MG ( $P > 0.05$ ) (Figure 8B). Of note, the reconstructed core lncRNA-miRNA-mRNA networks showed that the lncRNA-LOC102550026 cluster consisted of 2 miRNAs and 5 mRNAs (Figure 8C). We further validated 2 miRNAs and 5 mRNAs by qRT-PCR (Figure 8D-J). The results of miRNA-34c-5p and Pck1 mRNA transcriptions were consistent with the sequencing data ( $p < 0.05$ ) (Figure 8E and F).

Moreover, Western blot analysis (Figure 8M and N) showed that compared with that in the NG, the protein expression of Pck1 was significantly decreased in the MG ( $P < 0.05$ ). Compared with that in the MG, the protein expression of Pck1 was significantly increased in the HPMG ( $P < 0.01$ ). The result was in accordance with PCR data. Using the Miranda program to predict targeting relationship among lncRNA-miRNA-mRNA sequences, we found that lncRNA LOC102550026 can target with miRNA-34c-5p, and miRNA-34c-5p can target with Pck1 (Figure 8K and L).

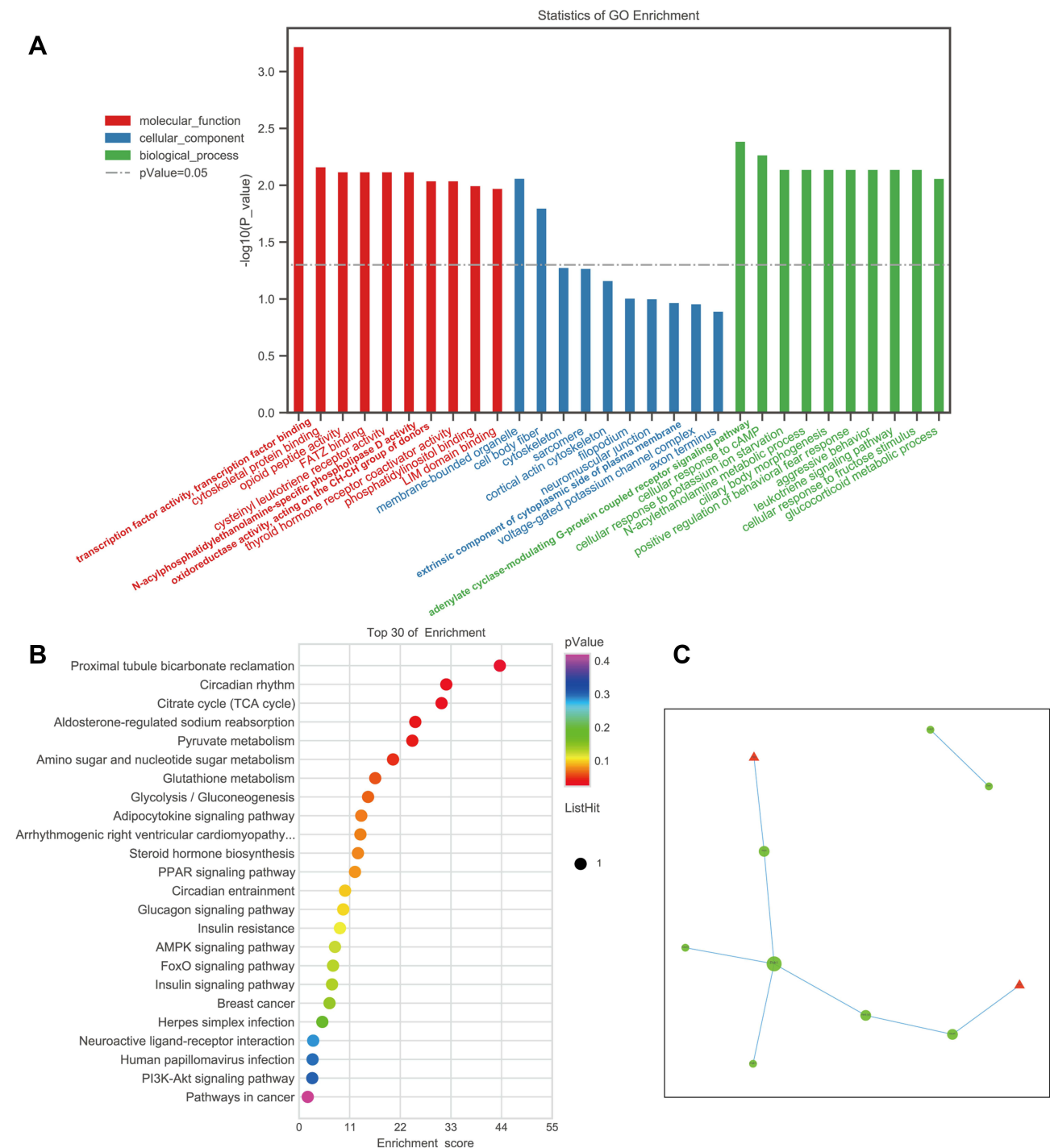


**Figure 7** Functional analysis of ceRNA network. **(A)** Top 10 GO terms of mRNAs in ceRNA networks. **(B)** Top 30 significant KEGG pathways of mRNAs in ceRNA networks. **(C)** PPI network construction for mRNA in ceRNA network. The value of centrality degree is marked by different node size. Up or down regulation of genes is filled with red or blue color, respectively.

## Discussion

Recently, studies are growing on the importance of lncRNAs in IBD.<sup>16,17</sup> The dysregulated lncRNAs and mRNAs were measured by RNA-seq analysis or microarray technology in colitis mice or IBD patients.<sup>39,40</sup> A previous study discovered that lnc-ITSN1-2/miR-125a/IL-23R axis promoted CD4<sup>+</sup> T cell activation and Th1/Th17 cell differentiation in IBD.<sup>41</sup> HPM, as a type of moxibustion, has the functions of dispelling cold, warmly lubricating, and improving the

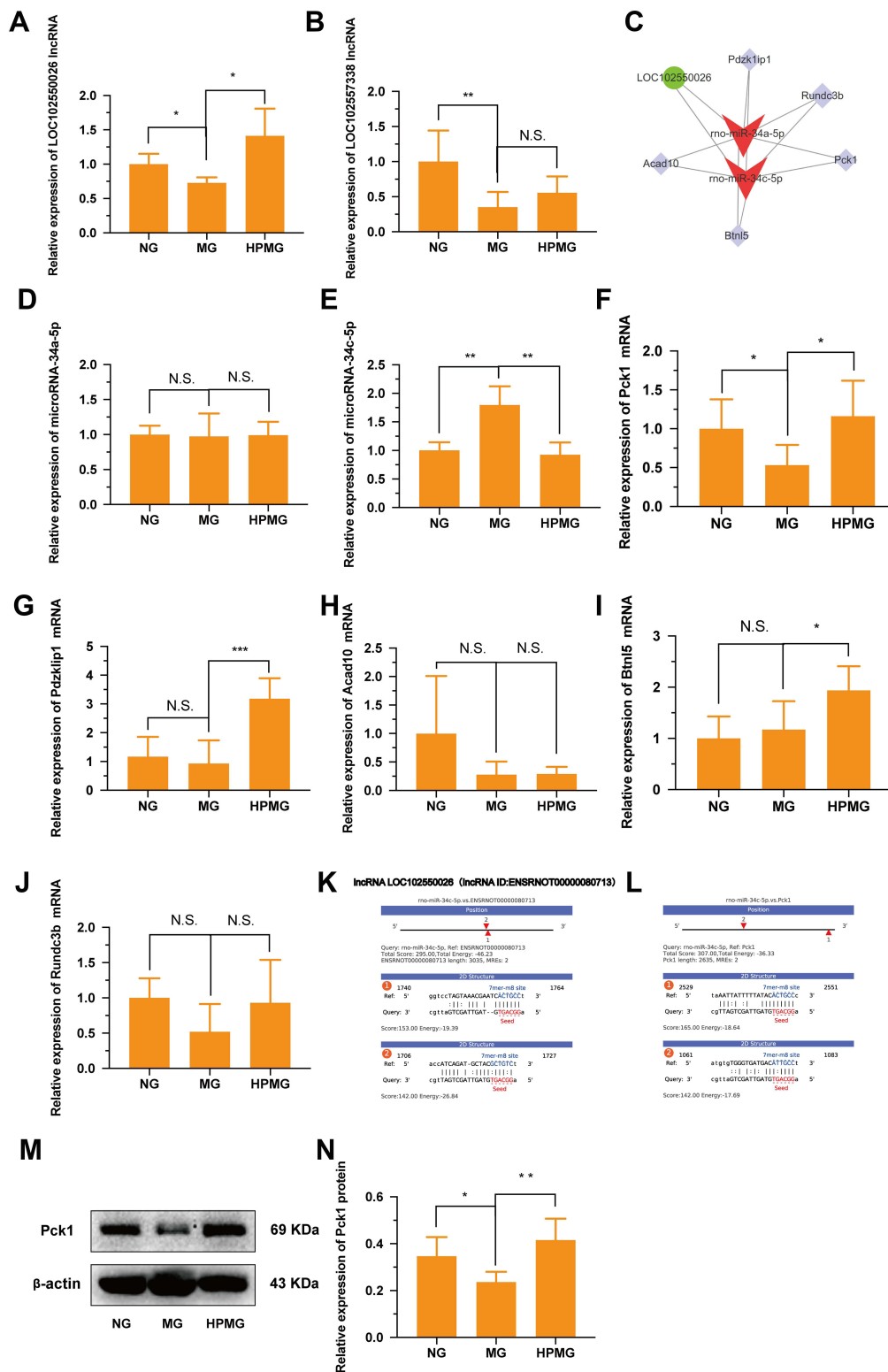


**Figure 8** Validations of the selected DE RNA expression. **(A and B)** The key lncRNAs expressions of LOC102550026 and LOC102557338 were measured by qRT-PCR (n = 6). **(C)** The core lncRNA-miRNA-mRNA network analysis. **(D and E)** The expressions of miRNA-34a-5p and miRNA-34c-5p were measured by qRT-PCR (n = 6). **(F-J)** The mRNA expressions of Pck1, pdzklp1, Acad10, Btl5 and Runc3b were measured by qRT-PCR (n = 6). **(K)** The targeting relationship between lncRNA-LOC102550026 and miRNA-34c-5p was predicted. **(L)** The targeting relationship between miRNA-34c-5p and Pck1 was predicted. **(M and N)** Western blot analysis of Pck1 protein in colon homogenate in each group. Data are expressed as mean ± standard deviation. \*p < 0.05, \*\*p < 0.01, \*\*\*p < 0.001.

**Abbreviations:** DE, differentially expressed; NG, control group; MG, model group; HPMG, herb-partitioned moxibustion group.

function of meridians, and has been widely used in the treatment of various diseases.<sup>42–44</sup> It has been suggested that HPM is effective in treating CD patients.<sup>45,46</sup> However, whether HPM can regulate lncRNAs in CD development and progression is still vastly unknown, and the role of HPM in regulating ceRNA in the development of CD has not been comprehensively explored. In the previous study, we confirmed that HPM treatment (at Qihai (CV 6) and Tianshu (ST 25)) promoted the repair of injured mucosa in CD rats.<sup>47</sup> Thus, in this study, the CD rats were treated with HPM (at Qihai (CV 6) and bilateral Tianshu (ST 25)). Subsequently, we detected lncRNA miRNA and mRNA expression profiles in NG, MG and HPMG rats.

The RNA-seq analysis exhibited that 189 lncRNAs were significantly differentially expressed in the MG compared to the NG (Figure 3A and B). GO analysis suggested that the DE lncRNAs were mostly associated with the regulation of epithelial cell proliferation and mitochondrial matrix (Figure 3C). There are many intestinal epithelial cells in the intestinal lumen, and this barrier of intestinal epithelial cells acts as the first physical and immunological protective wall.<sup>48</sup> Increased apoptosis was reported in the intestinal epithelium in CD patients.<sup>49</sup> It has been reported that mitochondrial energy function and gut bacteria in most tissues may be interdependent. Intestinal bacterial signals may affect mitochondrial function, and in return, mediators released by mitochondrial-regulated tissues (such as endocrine, immune) may affect the gut microbiota.<sup>50</sup> The KEGG pathways were mainly related to PI3K-Akt signaling pathway, mTOR signaling pathway, NF- $\kappa$ B signaling pathway and Ras signaling pathway (Figure 3D). The previous sequencing results also pointed out that the enriched KEGG pathways in CD included PI3K-Akt signaling pathway and mTOR signaling pathway.<sup>51–53</sup> It has been proved that CD promotes the activation of NF- $\kappa$ B and Ras.<sup>54,55</sup> Together, these data indicated that the lncRNAs play a critical role in CD pathogenesis.

Our results further indicated that 161 lncRNAs were significantly differentially expressed in the HPMG compared to the MG (Figure 4A and B). GO enrichment analysis disclosed that DE lncRNAs in the HPMG were enriched in TOR signaling, extracellular matrix, G-protein coupled receptor activity and ATPase binding (Figure 4C). The TOR signaling has been reported to be related to CD,<sup>53</sup> and due to extensive mucosal remodeling, the extracellular matrix remodeling of intestinal tissue is important in IBD.<sup>56</sup> It is suggested that G protein-coupled receptors have been associated with the development of IBD and play an important role in regulating intestinal functions.<sup>57,58</sup> These implied that HPM may reduce colonic mucosal damage by regulating TOR signaling, extracellular matrix and G protein-coupled receptors in CD. Our previous study has further pointed out that ATP content in colon tissues was considerably increased in CD rats. Conversely, HPM treatment can reduce ATP content in the colon tissues.<sup>47</sup> In addition, the KEGG pathways were mainly related to cell adhesion molecules and PI3K-Akt signaling pathway (Figure 4D). Due to the loss of growth factors or cell adhesion molecules, the normal healing process of mucosal may be disrupted by pathophysiological conditions (such as inflammation).<sup>59</sup> Our RNA-seq results suggested that the PI3K-Akt signaling pathway is co-expressed in KEGG pathway analysis of NG, MG and HPMG (Figures 3D and 4D). Therefore, the KEGG results reflect the potential mechanism of HPM in the treatment in CD rats, which is by regulating cell adhesion molecules and PI3K-Akt signaling pathway. In total, we identified 32 DE miRNAs and 463 DE mRNAs in CD versus normal control rats, and 12 DE miRNAs and 259 DE mRNAs in HPM versus CD rats via small RNA and RNA sequencing data (Figure 5). The miRNAs and mRNAs related GO analysis and KEGG pathway analysis are listed in [Supplementary Figure 1-4](#).

Recent research has shown that lncRNAs can act as ceRNAs to protect mRNAs from miRNA inhibition.<sup>60,61</sup> Then, we constructed a ceRNA network to understand the function of lncRNAs (Figure 6). Furthermore, GO analysis found that cAMP was involved in CD pathogenesis, as confirmed by previous publications.<sup>62</sup> Whereas, in KEGG pathway analysis, the main pathways identified included pyruvate metabolism, glycolysis/gluconeogenesis, adipocytokine signaling pathway, PPAR signaling pathway, AMPK signaling pathway, FoxO signaling pathway and PI3K-Akt signaling pathway (Figure 7B).

Based on previous findings, pyruvate metabolism and glycolysis/gluconeogenesis are critical for the development of inflammatory bowel disease.<sup>63,64</sup> In pathological states, the strong correlation between adipocytokine level and inflammation severity is demonstrated in IBD.<sup>65</sup> Decreased expression of PPAR gamma may cause persistent mucosal inflammation in colitis. Up regulation of PPAR gamma may play an anti-inflammatory role in IBD.<sup>66</sup> It is reported that intestinal fibrosis is

alleviated by enhancing the phosphorylation of AMPK in CD,<sup>67</sup> and previous bioinformatics analysis also identified MAPK signaling and PI3K-Akt signaling as crucial signaling pathways for Crohn's Disease.<sup>52</sup> Another bioinformatics analysis study showed that the levels of autophagy-related proteins in FoxO signaling pathway were higher, but the levels of proteins related to inflammation in the intestinal mucosa were reduced.<sup>68</sup> FoxO4 transcription is temporarily suppressed in TNBS treatment and IBD patients.<sup>69</sup> These studies are in accordance with our bioinformatic analysis, and HPM may regulate adipocytokine, PPAR, AMPK, FoxO and PI3K-Akt signaling pathway to regulate the intestinal inflammation in CD.

In the present study, we chose the 2 lncRNAs with the highest ceRNA scores for validation. The expressions of LOC102550026 and LOC102557338 were significantly decreased in the MG compared to the NG ( $p < 0.05$ ), while the LOC102550026 expression level was markedly increased in the HPMG than in the MG ( $p < 0.05$ ) (Figure 8A and B). The results demonstrated that the CD rats were treated with HPM by regulating lncRNA-LOC102550026. Therefore, we constructed the core lncRNA-miRNA-mRNA networks, and lncRNA-LOC102550026 cluster consisted of 2 miRNAs and 5 mRNAs (Figure 8C). We further validated 2 miRNAs and 5 mRNAs by qRT-PCR (Figure 8D–J). The results of miRNA-34c-5p and Pck1 mRNA transcriptions were consistent with the sequencing data ( $p < 0.05$ ) (Figure 8E and F). Moreover, Western blot result of Pck1 (Figure 8M and N) was in accordance with PCR data. It's implied that lncRNA-LOC102550026 might be involved in inflammatory response via miRNA-34c-5p/Pck1 axis in CD, and HPM may treat CD through regulating the lncRNA-LOC102550026/miRNA-34c-5p/Pck1 axis.

Recently, a study showed that inhibition of miR-34c-5p could reduce neuropathic pain and inflammation by up-regulating SIRT1 and blocking the STAT3 signaling pathway,<sup>70</sup> but miR-34c-5p in CD was not reported. Phosphoenolpyruvate carboxykinase 1 (Pck1) is well-known for its function as a gluconeogenic enzyme.<sup>71</sup> The Pck1 deletion in macrophages increased reactive oxygen species and cytokines TNF $\alpha$ , IL-1 $\beta$ , and IL-6 expressions, and contributed to M1 polarization. These indicated that Pck1 deletion increased the proinflammatory phenotype in macrophages.<sup>72</sup> It has been reported that inflammatory factor CXCL8 can be inhibited by upregulating Pck1 in ulcerative colitis (UC).<sup>73</sup> Upregulating Pck1 during the peripartal period improved liver function and reduced inflammation and oxidative stress.<sup>74</sup> Additionally, we performed a PPI net analysis to investigate mRNAs' CD influences (Figure 7C). We further identified one key hub gene, namely, Pck1, through the PPI network. However, the functions of Pck1 in CD were not reported previously. Therefore, according to ceRNA and KEGG analyses, we propose that the lncRNA LOC102550026/miRNA-34c-5p/Pck1 axis and adipocytokine, PPAR, AMPK, FoxO, and PI3K-Akt signaling pathways may regulate the intestinal immune-inflammatory response (Figure 9A), and HPM may regulate the lncRNA LOC102550026/miRNA-34c-5p/Pck1 axis and adipocytokine, PPAR, AMPK, FoxO, and PI3K-Akt signaling pathways to improve intestinal inflammation in CD (Figure 9B). However, this study has several limitations. First, we only predicted the potential roles of lncRNA-miRNA-mRNA network and related regulatory pathways by bioinformatics analysis in CD, but the results need to be further validated with related experiments. Second, RNA-seq and miRNA-seq were performed on total colon tissues containing multiple cell types; thus, we need further study to determine the roles of lncRNAs in specific cell types. Third, the sample size is small for RNA sequencing, which may affect the extrapolation accuracy of the results. A larger sample size is needed to verify the results.

## Conclusion

In general, we identified the expression profiles of lncRNAs, miRNAs, and mRNAs in CD, and we found that lncRNA-LOC102550026 and lncRNA-LOC102557338 might play critical roles in the pathogenesis of CD. In addition, this study is the first study to identify lncRNAs, miRNAs, and mRNAs profiles after HPM treatment in CD for the first time. By constructing a ceRNA network with lncRNA-miRNA-mRNA, PCR verification, and KEGG analysis, we identified that HPM might regulate the lncRNA LOC102550026/miR-34c-5p/Pck1 axis and adipocytokine, PPAR, AMPK, FoxO, and PI3K-Akt signaling pathways to improve intestinal inflammation in CD. However, further studies are required to verify if HPM regulates adipocytokine, PPAR, AMPK, FoxO, and PI3K-Akt signaling pathways by affecting lncRNA LOC102550026/miR-34c-5p/Pck1 axis. In all, our findings offered new insights for HPM treatment into the molecular mechanisms in CD.

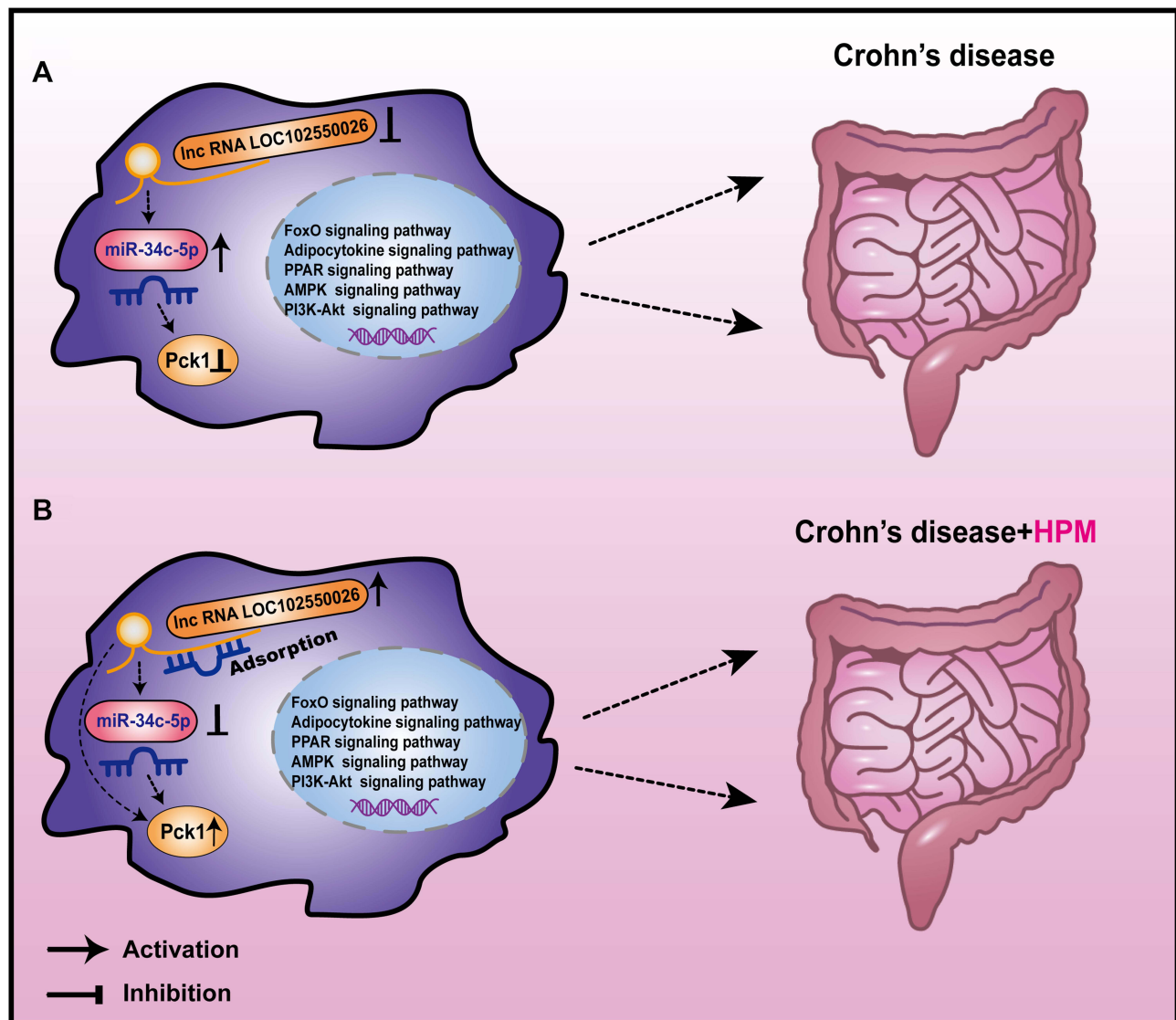


**Figure 9** Schematic diagram illustrating the mechanism. LncRNA LOC102550026/miRNA-34c-5p/Pck1 axis and adipocytokine, PPAR, AMPK, FoxO and PI3K-Akt signaling pathways may regulate the intestinal immune inflammatory response (A), and HPM may regulate the LncRNA LOC102550026/miRNA-34c-5p/Pck1 axis and adipocytokine, PPAR, AMPK, FoxO and PI3K-Akt signaling pathways to improve intestinal inflammation in CD (B).

**Abbreviation:** HPM, herb-partitioned moxibustion.

## Data Sharing Statement

All relevant data have been provided in the manuscript.

## Author Contributions

All authors made a significant contribution to the work reported, whether that is in the conception, study design, execution, acquisition of data, analysis and interpretation, or in all these areas; took part in drafting, revising or critically reviewing the article; gave final approval of the version to be published; have agreed on the journal to which the article has been submitted; and agree to be accountable for all aspects of the work.

## Funding

This work was supported by National Natural Science Foundation of China (No.81674073, No. 81273843); Natural Science Foundation of Shanghai (No. 20ZR1453000, No. 19ZR1451600); and Outstanding Discipline Leader Plan of Shanghai Health and Family Planning System (No. 2017BR047).

## Disclosure

The authors declare that they have no conflicts of interest for this work.

## References

- Roda G, Chien NS, Kotze PG, et al. Crohn's disease. *Nat Rev Dis Primers*. 2020;6(1):22. doi:10.1038/s41572-020-0156-2
- Ng SC, Shi HY, Hamidi N, et al. Worldwide incidence and prevalence of inflammatory bowel disease in the 21st century: a systematic review of population-based studies. *Lancet*. 2017;390(10114):2769–2778. doi:10.1016/s0140-6736(17)32448-0
- Torres J, Mehandru S, Colombel JF, Peyrin-Biroulet L. Crohn's disease. *Lancet*. 2017;389(10080):1741–1755. doi:10.1016/s0140-6736(16)31711-1
- Kaser A, Zeissig S, Blumberg RS. Inflammatory bowel disease. *Annu Rev Immunol*. 2010;28:573–621. doi:10.1146/annurev-immunol-030409-101225
- Zhang YZ, Li YY. Inflammatory bowel disease: pathogenesis. *World J Gastroenterol*. 2014;20(1):91–99. doi:10.3748/wjg.v20.i1.91
- Gil N, Ulitsky I. Regulation of gene expression by cis-acting long non-coding RNAs. *Nat Rev Genet*. 2020;21(2):102–117. doi:10.1038/s41576-019-0184-5
- Quinn JJ, Chang HY. Unique features of long non-coding RNA biogenesis and function. *Nat Rev Genet*. 2016;17(1):47–62. doi:10.1038/nrg.2015.10
- Michalik KM, You X, Manavski Y, et al. Long noncoding RNA MALAT1 regulates endothelial cell function and vessel growth. *Circ Res*. 2014;114(9):1389–1397. doi:10.1161/circresaha.114.303265
- Huang MD, Chen WM, Qi FZ, et al. Long non-coding RNA ANRIL is upregulated in hepatocellular carcinoma and regulates cell proliferation by epigenetic silencing of KLF2. *J Hematol Oncol*. 2015;8(1):57. doi:10.1186/s13045-015-0153-1
- Li Z, Chao TC, Chang KY, et al. The long noncoding RNA THRIL regulates TNF $\alpha$  expression through its interaction with hnRNPL. *Proc Natl Acad Sci U S A*. 2014;111(3):1002–1007. doi:10.1073/pnas.1313768111
- Cesana M, Cacchiarelli D, Legnini I, et al. A long noncoding RNA controls muscle differentiation by functioning as a competing endogenous RNA. *Cell*. 2011;147(2):358–369. doi:10.1016/j.cell.2011.09.028
- Salmena L, Poliseno L, Tay Y, Kats L, Pandolfi PP. A ceRNA hypothesis: the Rosetta Stone of a hidden RNA language? *Cell*. 2011;146(3):353–358. doi:10.1016/j.cell.2011.07.014
- Wang J, Yan S, Yang J, Lu H, Xu D, Wang Z. Non-coding RNAs in Rheumatoid Arthritis: from Bench to Bedside. *Front Immunol*. 2019;10:3129. doi:10.3389/fimmu.2019.03129
- Li Y, Zhang S, Zhang C, Wang M. LncRNA MEG3 inhibits the inflammatory response of ankylosing spondylitis by targeting miR-146a. *Mol Cell Biochem*. 2020;466(1–2):17–24. doi:10.1007/s11010-019-03681-x
- Tian F, Wang J, Zhang Z, Yang J. LncRNA SNHG7/miR-34a-5p/SYVN1 axis plays a vital role in proliferation, apoptosis and autophagy in osteoarthritis. *Biol Res*. 2020;53(1):9. doi:10.1186/s40659-020-00275-6
- Ghafouri-Fard S, Eghtedarian R, Taheri M. The crucial role of non-coding RNAs in the pathophysiology of inflammatory bowel disease. *Biomed Pharmacother*. 2020;129:110507. doi:10.1016/j.biopha.2020.110507
- Qiao YQ, Huang ML, Xu AT, Zhao D, Ran ZH, Shen J. LncRNA DQ786243 affects Treg related CREB and Foxp3 expression in Crohn's disease. *J Biomed Sci*. 2013;20(1):87. doi:10.1186/1423-0127-20-87
- Haberman Y, BenShoshan M, Di Segni A, et al. Long ncRNA Landscape in the Ileum of Treatment-Naive Early-Onset Crohn Disease. *Inflamm Bowel Dis*. 2018;24(2):346–360. doi:10.1093/ibd/izx013
- Li Y, Zhu L, Chen P, et al. MALAT1 maintains the intestinal mucosal homeostasis in Crohn's disease via the miR-146b-5p-CLDN11/NUMB pathway. *J Crohns Colitis*. 2021. doi:10.1093/ecco-jcc/jjab040
- Bao CH, Wu LY, Shi Y, et al. Moxibustion down-regulates colonic epithelial cell apoptosis and repairs tight junctions in rats with Crohn's disease. *World J Gastroenterol*. 2011;17(45):4960–4970. doi:10.3748/wjg.v17.i45.4960
- Zhou J, Wu LY, Chen L, et al. Herbs-partitioned moxibustion alleviates aberrant intestinal epithelial cell apoptosis by upregulating A20 expression in a mouse model of Crohn's disease. *World J Gastroenterol*. 2019;25(17):2071–2085. doi:10.3748/wjg.v25.i17.2071
- Shi Y, Guo Y, Zhou J, et al. Herbs-partitioned moxibustion improves intestinal epithelial tight junctions by upregulating A20 expression in a mouse model of Crohn's disease. *Biomed Pharmacother*. 2019;118:109149. doi:10.1016/j.biopha.2019.109149
- Bao CH, Wu LY, Wu HG, et al. Moxibustion inhibits apoptosis and tumor necrosis factor- $\alpha$ /tumor necrosis factor receptor 1 in the colonic epithelium of Crohn's disease model rats. *Dig Dis Sci*. 2012;57(9):2286–2295. doi:10.1007/s10620-012-2161-0
- Zhao JM, Liu YN, Zheng HD, et al. Effect of Herb-Partitioned Moxibustion on Autophagy and Immune-Associated Gene Expression Profiles in a Rat Model of Crohn's Disease. *Evid Based Complement Alternat Med*. 2019;2019:3405146. doi:10.1155/2019/3405146
- Morris GP, Beck PL, Herridge MS, Depew WT, Szewczuk MR, Wallace JL. Hapten-induced model of chronic inflammation and ulceration in the rat colon. *Gastroenterology*. 1989;96(3):795–803.
- Okayasu I, Hatakeyama S, Yamada M, Ohkusa T, Inagaki Y, Nakaya R. A novel method in the induction of reliable experimental acute and chronic ulcerative colitis in mice. *Gastroenterology*. 1990;98(3):694–702. doi:10.1016/0016-5085(90)90290-h
- Wallace JL, Keenan CM, Gale D, Shoupe TS. Exacerbation of experimental colitis by nonsteroidal anti-inflammatory drugs is not related to elevated leukotriene B4 synthesis. *Gastroenterology*. 1992;102(1):18–27. doi:10.1016/0016-5085(92)91779-4
- Pertea M, Pertea GM, Antonescu CM, Chang TC, Mendell JT, Salzberg SL. StringTie enables improved reconstruction of a transcriptome from RNA-seq reads. *Nat Biotechnol*. 2015;33(3):290–295. doi:10.1038/nbt.3122
- Finn RD, Mistry J, Schuster-Böckler B, et al. Pfam: clans, web tools and services. *Nucleic Acids Res*. 2006;34(Database issue):D247–251. doi:10.1093/nar/gkj149
- Li A, Zhang J, Zhou Z. PLEK: a tool for predicting long non-coding RNAs and messenger RNAs based on an improved k-mer scheme. *BMC Bioinform*. 2014;15(1):311. doi:10.1186/1471-2105-15-311
- Sun L, Liu H, Zhang L, Meng J. lncRScan-SVM: a Tool for Predicting Long Non-Coding RNAs Using Support Vector Machine. *PLoS One*. 2015;10(10):e0139654. doi:10.1371/journal.pone.0139654



32. Altschul SF, Gish W, Miller W, Myers EW, Lipman DJ. Basic local alignment search tool. *J Mol Biol.* 1990;215(3):403–410. doi:10.1016/s0022-2836(05)80360-2
33. Griffiths-Jones S, Bateman A, Marshall M, Khanna A, Eddy SR. Rfam: an RNA family database. *Nucleic Acids Res.* 2003;31(1):439–441. doi:10.1093/nar/gkg006
34. Griffiths-Jones S, Saini HK, Van Dongen S, Enright AJ. miRBase: tools for microRNA genomics. *Nucleic Acids Res.* 2008;36(Databaseissue):D154–158. doi:10.1093/nar/gkm952
35. Friedländer MR, Mackowiak SD, Li N, Chen W, Rajewsky N. miRDeep2 accurately identifies known and hundreds of novel microRNA genes in seven animal clades. *Nucleic Acids Res.* 2012;40(1):37–52. doi:10.1093/nar/gkr688
36. Guo L, Yu J, Liang T, Zou Q. miR-isomiRExp: a web-server for the analysis of expression of miRNA at the miRNA/isomiR levels. *Sci Rep.* 2016;6:23700. doi:10.1038/srep23700
37. Tino P. Basic properties and information theory of Audic-Claverie statistic for analyzing cDNA arrays. *BMC Bioinform.* 2009;10:310. doi:10.1186/1471-2105-10-310
38. Szklarczyk D, Gable AL, Lyon D, et al. STRING v11: protein-protein association networks with increased coverage, supporting functional discovery in genome-wide experimental datasets. *Nucleic Acids Res.* 2019;47(D1):D607–d613. doi:10.1093/nar/gky1131
39. Li N, Shi R. Expression alteration of long non-coding RNAs and their target genes in the intestinal mucosa of patients with Crohn's disease. *Clin Chim Acta.* 2019;494:14–21. doi:10.1016/j.cca.2019.02.031
40. Rankin CR, Theodorou E, Man Law IK, et al. Identification of novel mRNAs and lncRNAs associated with mouse experimental colitis and human inflammatory bowel disease. *Am J Physiol Gastrointest Liver Physiol.* 2018;315(5):G722–g733. doi:10.1152/ajpgi.00077.2018
41. Nie J, Zhao Q. Lnc-ITSN1-2, Derived From RNA Sequencing, Correlates With Increased Disease Risk, Activity and Promotes CD4(+) T Cell Activation, Proliferation and Th1/Th17 Cell Differentiation by Serving as a ceRNA for IL-23R via Sponging miR-125a in Inflammatory Bowel Disease. *Front Immunol.* 2020;11:852. doi:10.3389/fimmu.2020.00852
42. Qi Q, Im H, Li KS, et al. Influence of herb-partitioned moxibustion at Qihai (CV6) and bilateral Tianshu (ST25) and Shangjuxu (ST37) acupoints on toll-like receptors 4 signaling pathways in patients with ulcerative coliti. *J Tradit Chin Med.* 2021;41(3):479–485. doi:10.19852/j.cnki.jtcm.20210310.001
43. Liu Y, Sun J, Wang X, Shi L, Yan Y. Effect of herb-partitioned moxibustion for primary dysmenorrhea: a randomized clinical trial. *J Tradit Chin Med.* 2019;39(2):237–245.
44. Hu H, Chen L, Jin X, Li R, Fang J. Effect of herb-partitioned moxibustion on pain and quality of life in women with endometriosis: a protocol for a randomized clinical trial. *J Tradit Chin Med.* 2020;40(2):324–332.
45. Joos S, Brinkhaus B, Maluche C, et al. Acupuncture and moxibustion in the treatment of active Crohn's disease: a randomized controlled study. *Digestion.* 2004;69(3):131–139. doi:10.1159/000078151
46. Bao CH, Zhao JM, Liu HR, et al. Randomized controlled trial: moxibustion and acupuncture for the treatment of Crohn's disease. *World J Gastroenterol.* 2014;20(31):11000–11011. doi:10.3748/wjg.v20.i31.11000
47. Zhang J, Wang XJ, Wu LJ, et al. Herb-partitioned moxibustion alleviates colonic inflammation in Crohn's disease rats by inhibiting hyperactivation of the NLRP3 inflammasome via regulation of the P2X7R-Pannexin-1 signaling pathway. *PLoS One.* 2021;16(5):e0252334. doi:10.1371/journal.pone.0252334
48. Turner JR. Intestinal mucosal barrier function in health and disease. *Nat Rev Immunol.* 2009;9(11):799–809. doi:10.1038/nri2653
49. Di sabatino A, Ciccocioppo R, Luinetti O, et al. Increased enterocyte apoptosis in inflamed areas of Crohn's disease. *Dis Colon Rectum.* 2003;46(11):1498–1507. doi:10.1007/s10350-004-6802-z
50. Ruiz E, Penrose HM, Heller S, et al. Bacterial TLR4 and NOD2 signaling linked to reduced mitochondrial energy function in active inflammatory bowel disease. *Gut Microbes.* 2020;11(3):350–363. doi:10.1080/19490976.2019.1611152
51. Cheng C, Hua J, Tan J, Qian W, Zhang L, Hou X. Identification of differentially expressed genes, associated functional terms pathways, and candidate diagnostic biomarkers in inflammatory bowel diseases by bioinformatics analysis. *Exp Ther Med.* 2019;18(1):278–288. doi:10.3892/etm.2019.7541
52. Li H, Li Q, Sun S, Lei P, Cai X, Shen G. Integrated Bioinformatics Analysis Identifies ELAVL1 and APP as Candidate Crucial Genes for Crohn's Disease. *J Immunol Res.* 2020;2020:3067273. doi:10.1155/2020/3067273
53. Yin J, Hu T, Xu L, et al. Circular RNA expression profile in peripheral blood mononuclear cells from Crohn disease patients. *Medicine.* 2019;98(26):e16072. doi:10.1097/md.00000000000016072
54. Tawfik A, Knight P, Duckworth CA, Pritchard DM, Rhodes JM, Campbell BJ. Replication of Crohn's Disease Mucosal E. coli Isolates inside Macrophages Correlates with Resistance to Superoxide and Is Dependent on Macrophage NF-kappa B Activation. *Pathogens.* 2019;8(2). doi:10.3390/pathogens8020074
55. Wang X, Lu Y, Wu L, et al. Moxibustion Inhibits the ERK Signaling Pathway and Intestinal Fibrosis in Rats with Crohn's Disease. *Evid Based Complement Alternat Med.* 2013;2013:198282. doi:10.1155/2013/198282
56. Mortensen JH, Lindholm M, Langholm LL, et al. The intestinal tissue homeostasis - the role of extracellular matrix remodeling in inflammatory bowel disease. *Expert Rev Gastroenterol Hepatol.* 2019;13(10):977–993. doi:10.1080/17474124.2019.1673729
57. Lee T, Lee E, Arrollo D, Lucas PC, Parameswaran N. Non-Hematopoietic  $\beta$ -Arrestin1 Confers Protection Against Experimental Colitis. *J Cell Physiol.* 2016;231(5):992–1000. doi:10.1002/jcp.25216
58. Wang Y, de Vallière C, Imenez Silva PH, et al. The Proton-activated Receptor GPR4 Modulates Intestinal Inflammation. *J Crohns Colitis.* 2018;12(3):355–368. doi:10.1093/ecco-jcc/jjx147
59. Day R, Forbes A. Heparin, cell adhesion, and pathogenesis of inflammatory bowel disease. *Lancet.* 1999;354(9172):62–65. doi:10.1016/s0140-6736(98)09267-8
60. Su Z, Zhi X, Zhang Q, Yang L, Xu H, Xu Z. LncRNA H19 functions as a competing endogenous RNA to regulate AQP3 expression by sponging miR-874 in the intestinal barrier. *FEBS Lett.* 2016;590(9):1354–1364. doi:10.1002/1873-3468.12171
61. Tay Y, Rinn J, Pandolfi PP. The multilayered complexity of ceRNA crosstalk and competition. *Nature.* 2014;505(7483):344–352. doi:10.1038/nature12986
62. Li H, Zuo J, Tang W. Phosphodiesterase-4 Inhibitors for the Treatment of Inflammatory Diseases. *Front Pharmacol.* 2018;9:1048. doi:10.3389/fphar.2018.01048

63. Czub E, Nowak JK, Szaflarska-Poplawska A, et al. Comparison of fecal pyruvate kinase isoform M2 and calprotectin in assessment of pediatric inflammatory bowel disease severity and activity. *Acta Biochim Pol.* 2014;61(1):99–102.
64. Winkelmann P, Unterweger AL, Khullar D, et al. The PI3K pathway as a therapeutic intervention point in inflammatory bowel disease. *Immun Inflamm Dis.* 2021;9(3):804–818. doi:10.1002/iid3.435
65. Bilski J, Mazur-Bialy A, Wojcik D, et al. Role of Obesity, Mesenteric Adipose Tissue, and Adipokines in Inflammatory Bowel Diseases. *Biomolecules.* 2019;9:12. doi:10.3390/biom9120780
66. Han X, Benight N, Osuntokun B, Loesch K, Frank SJ, Denson LA. Tumour necrosis factor alpha blockade induces an anti-inflammatory growth hormone signalling pathway in experimental colitis. *Gut.* 2007;56(1):73–81. doi:10.1136/gut.2006.094490
67. Xie M, Xiong Z, Yin S, et al. Adiponectin Alleviates Intestinal Fibrosis by Enhancing AMP-Activated Protein Kinase Phosphorylation. *Dig Dis Sci.* 2021. doi:10.1007/s10620-021-07015-0
68. Cheng S, Ma X, Geng S, et al. Fecal Microbiota Transplantation Beneficially Regulates Intestinal Mucosal Autophagy and Alleviates Gut Barrier Injury. *mSystems.* 2018;3(5). doi:10.1128/mSystems.00137-18
69. Zhou W, Cao Q, Peng Y, et al. FoxO4 inhibits NF-kappaB and protects mice against colonic injury and inflammation. *Gastroenterology.* 2009;137(4):1403–1414. doi:10.1053/j.gastro.2009.06.049
70. Mo Y, Liu B, Qiu S, et al. Down-regulation of microRNA-34c-5p alleviates neuropathic pain via the SIRT1/STAT3 signaling pathway in rat models of chronic constriction injury of sciatic nerve. *J Neurochem.* 2020;154(3):301–315. doi:10.1111/jnc.14998
71. Beale EG, Harvey BJ, Forest C. PCK1 and PCK2 as candidate diabetes and obesity genes. *Cell Biochem Biophys.* 2007;48(2–3):89–95. doi:10.1007/s12013-007-0025-6
72. Ko CW, Counihan D, Wu J, Hatzoglou M, Puchowicz MA, Croniger CM. Macrophages with a deletion of the phosphoenolpyruvate carboxykinase 1 (Pck1) gene have a more proinflammatory phenotype. *J Biol Chem.* 2018;293(9):3399–3409. doi:10.1074/jbc.M117.819136
73. Guo H, Chi Y, Chi N. Bioinformatics analysis reveals possible molecular mechanism of PXR on regulating ulcerative colitis. *Sci Rep.* 2021;11(1):5428. doi:10.1038/s41598-021-83742-8
74. Batistel F, Osorio JS, Ferrari A, Trevisi E, Socha MT, Loor JJ. Immunometabolic Status during the Peripartum Period Is Enhanced with Supplemental Zn, Mn, and Cu from Amino Acid Complexes and Co from Co Glucoheptonate. *PLoS One.* 2016;11(5):e0155804. doi:10.1371/journal.pone.0155804

## Publish your work in this journal

The Journal of Inflammation Research is an international, peer-reviewed open-access journal that welcomes laboratory and clinical findings on the molecular basis, cell biology and pharmacology of inflammation including original research, reviews, symposium reports, hypothesis formation and commentaries on: acute/chronic inflammation; mediators of inflammation; cellular processes; molecular mechanisms; pharmacology and novel anti-inflammatory drugs; clinical conditions involving inflammation. The manuscript management system is completely online and includes a very quick and fair peer-review system. Visit <http://www.dovepress.com/testimonials.php> to read real quotes from published authors.

Submit your manuscript here: <https://www.dovepress.com/journal-of-inflammation-research-journal>